

Supporting information

**Scalable Synthesis of N-Doped Graphene-Oxide-Supported
FeCo(OH)_x Nanosheets for Efficient Co-Doped Fe₃O₄ Nanoparticle-
Based Oxygen Reduction Reaction Electrocatalysis**

Sunglun Kwon and Jong Hyeon Lee*

Department of Chemistry, The Catholic University of Korea, Bucheon, 14662 South Korea

S1. Materials and Methods

S1.1. Exfoliation of the layered double hydroxides

Synthesis of FeCo(OH)_x-NRGO: In a 25 mL Teflon-lined autoclave, dissolve 3.3 mM FeCl₂·4H₂O (99.99%, Sigma-Aldrich), 1.7 mM CoCl₂·6H₂O (98%, Sigma-Aldrich) (2:1 ratio), and 10 mg N-rGO (ACS material) in 18 mL formamide (98.5%, Junsei) and 2 mL ethanol (99.9%, Samchun Chemicals). The mixture is sonicated for 15 minutes to ensure thorough mixing. For solvothermal treatment, the mixed solution is transferred to the autoclave and heated at 120 °C for 6 hours under solvothermal conditions. After reaction, the reaction mixture is centrifuged at 4000 rpm for 7 minutes to collect the first precursor. The supernatant is discarded, and the precipitate is washed with degassed water and ethanol once each. The precipitate is dried in a vacuum pump for 5 hours. It is important to promptly wash the FeCo(OH)_x-NRGO, dry them under vacuum, and store them in a vacuum desiccator to minimize oxygen exposure. For the control experiment, we synthesized FeCo(OH)_x-NRGO samples with different the FeCl₂·4H₂O and CoCl₂·6H₂O ratios (3:0, 1:2, 1.5:1.5, 2:1 and 0:3) and adjusted the solvothermal reaction time to 3, 6, 9, and 12 hours.

Synthesis of (Co)Fe₃O₄-NRGO: The dried first precursor is placed in a tube furnace under Ar gas flow. The temperature is ramped up at a rate of 15 °C/min and maintained at 900 °C for 2 hours to obtain the (Co)Fe₃O₄-NRGO(900). To compare the samples, we calcined the (Co)Fe₃O₄-NRGO samples at 450, 600, 750, 900, 1050, and 1200 °C.

S1.2. Electrochemical measurements

Prior to catalyst ink loading, a 3 mm diameter glassy carbon (GC) working electrode was polished using 0.05 μm Al₂O₃ powder and subsequently rinsed with deionized water. 5 mg of the above-prepared samples, 1 mL deionized water, and 5 μL Nafion[®] solution (5 wt. % in lower aliphatic alcohols and water, Sigma–Aldrich) were placed in a vial, then sonicated to form a homogeneous

suspension. 5 μL of the catalyst ink was pipetted onto the surface of the GC electrode and allowed to dry for 10 minutes under vacuum conditions. Commercially available Pt/C catalyst (20 wt% Pt content, Pt Vulcan XC-72, Premetek) was used for this experiment. The electrochemical measurements were carried out using a CompactStat (Ivium Technologies) in a three-electrode configuration, where a glassy carbon electrode served as the working electrode, a Pt wire served as the counter electrode, and a saturated Ag/AgCl electrode served as the reference electrode. The cyclic voltammograms (CV) were measured in an O_2 - and N_2 -saturated KOH (0.1 M) solution at a scan rate of $50 \text{ mV}\cdot\text{s}^{-1}$. The RDE measurements were conducted in O_2 -saturated KOH (0.1 M) at a scan rate of $10 \text{ mV}\cdot\text{s}^{-1}$ and varying rotation rates from 400 to 3600 rpm. The K-L plots are a graphical representation of the K-L equation, which can be used to determine the electron transfer number for a given electrochemical reaction [1-3].

S1.3. General characterization

Scanning electron microscopy (SEM) images were acquired using a JSM-7800F Prime (JEOL). High-resolution transmission electron microscopy (HR-TEM) images were obtained using JEM-F200 and JEM-3010 instruments (JEOL). Crystalline structure analysis was conducted by X-ray diffraction (XRD) using a MiniFlex600 diffractometer (Cu $\text{K}\alpha$ radiation, $\lambda = 1.541 \text{ \AA}$). Thermal stability was investigated by thermogravimetric analysis (TGA) on a TGA 4000 instrument (Perkin Elmer) under a nitrogen atmosphere with a heating rate of $5 \text{ }^\circ\text{C}/\text{min}$ from room temperature to $900 \text{ }^\circ\text{C}$. X-ray photoelectron spectroscopy (XPS) was achieved through an ESCALAB 250. Elemental composition was further quantified by inductively coupled plasma atomic emission spectroscopy (ICP-AES) using an OPTIMA 8300 instrument (Perkin Elmer).

S2. Supporting figures

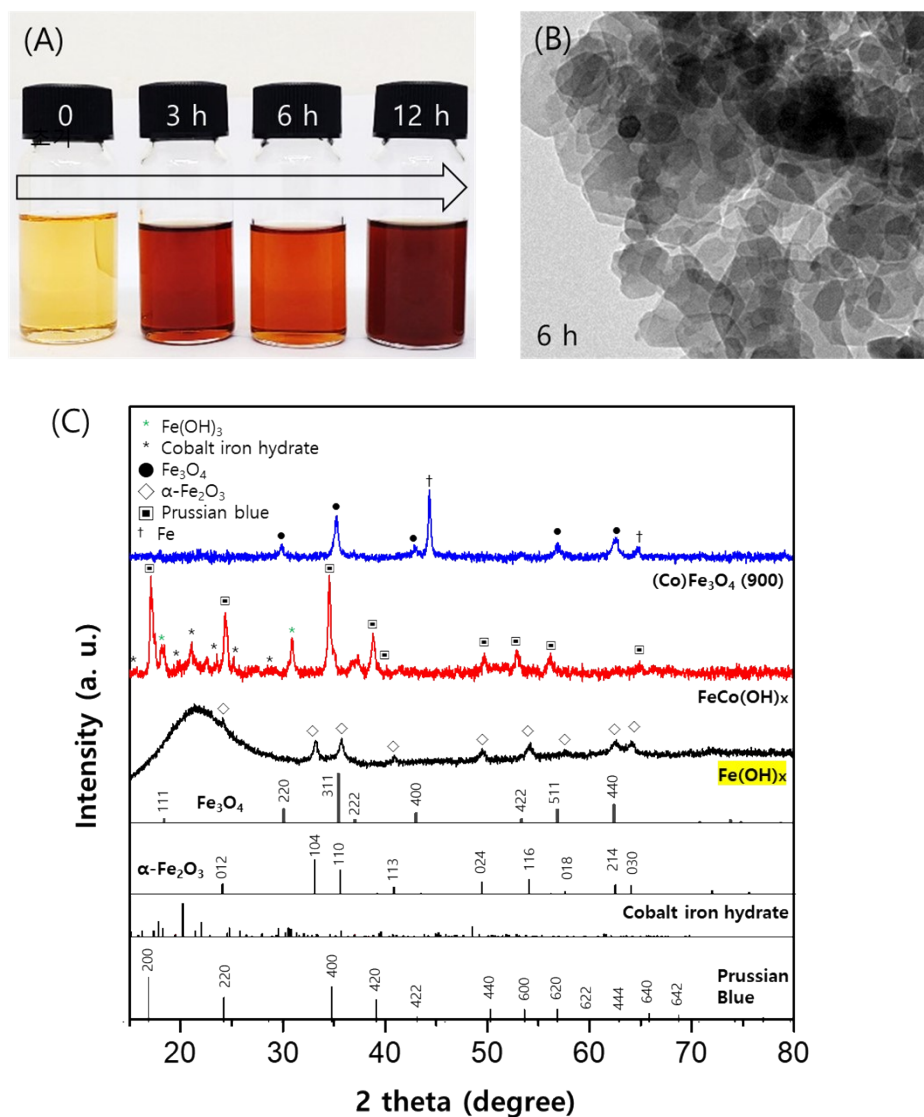


Figure S1. Solvothermal synthesis and characterization of FeCo(OH)_x and (Co)Fe₃O₄ without the support of NRGO: (A) Photographs of FeCo(OH)_x solutions after different solvothermal reaction times. (B) TEM image of FeCo(OH)_x nanoparticles synthesized via a 6-hour solvothermal reaction. (C) XRD patterns of Fe(OH)_x, FeCo(OH)_x via a 12-hour solvothermal reaction and (Co)Fe₃O₄. The (Co)Fe₃O₄ pattern corresponds to the product obtained after calcination of FeCo(OH)_x at 900°C.

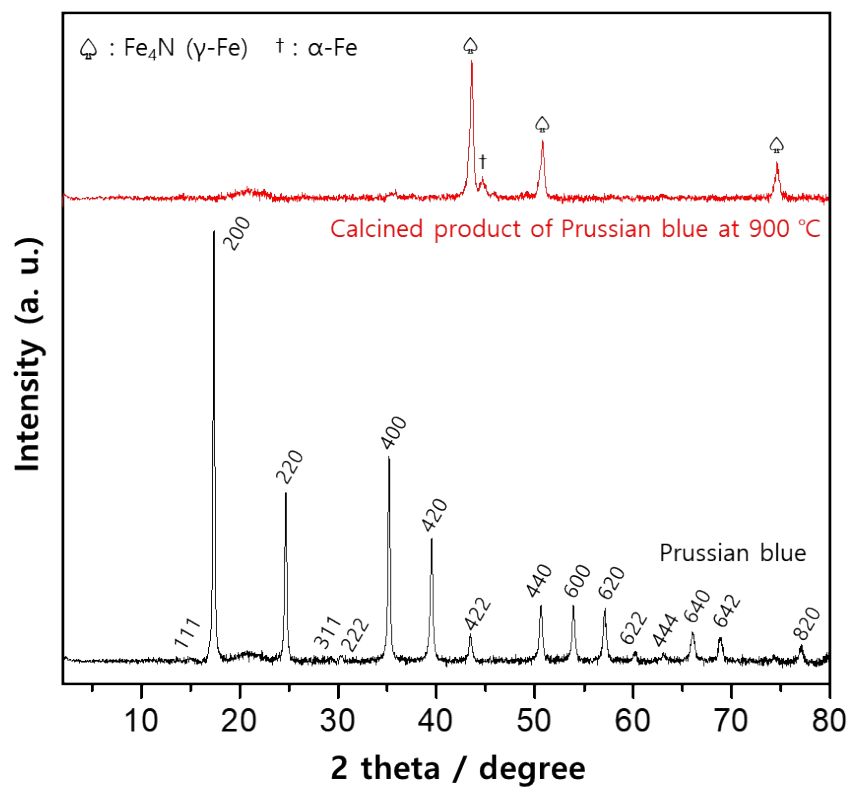


Figure S2. XRD pattern of commercial Prussian blue and calcined product of Prussian blue at 900 °C in Ar condition.

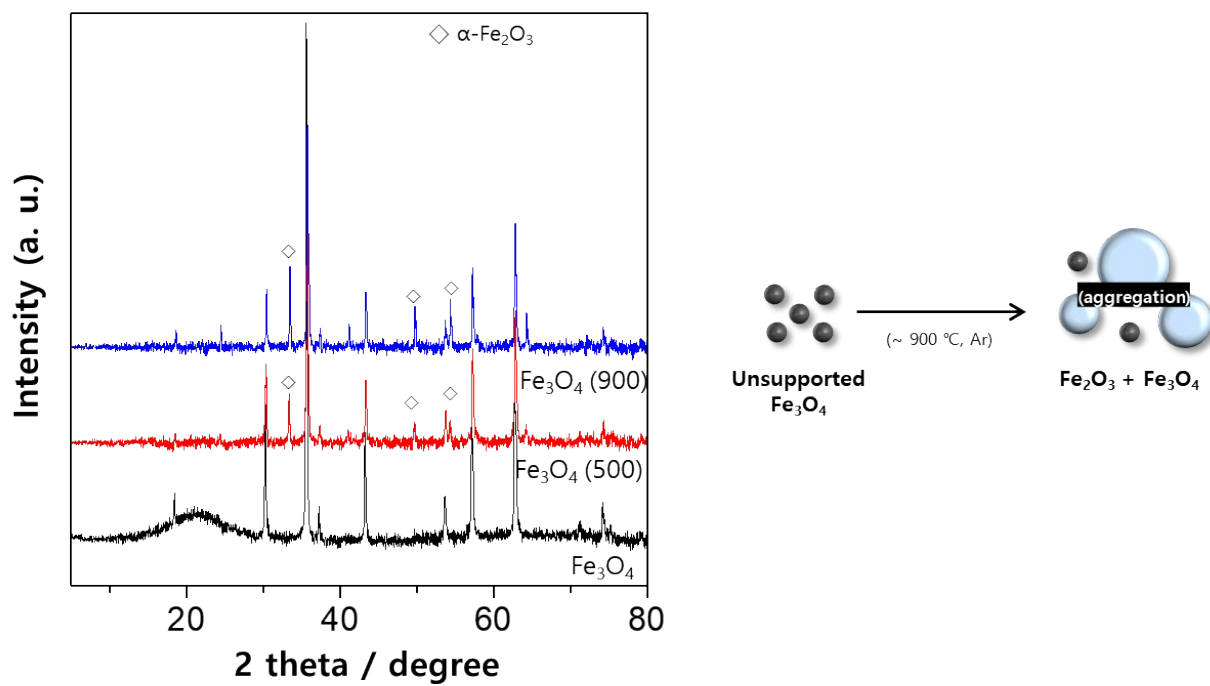


Figure S3. The XRD patterns of commercially available Fe_3O_4 nanoparticles (Alfa-aesar, 47141, 50-100 nm) and the Fe_3O_4 via calcination at 500°C and 900°C under argon atmosphere.

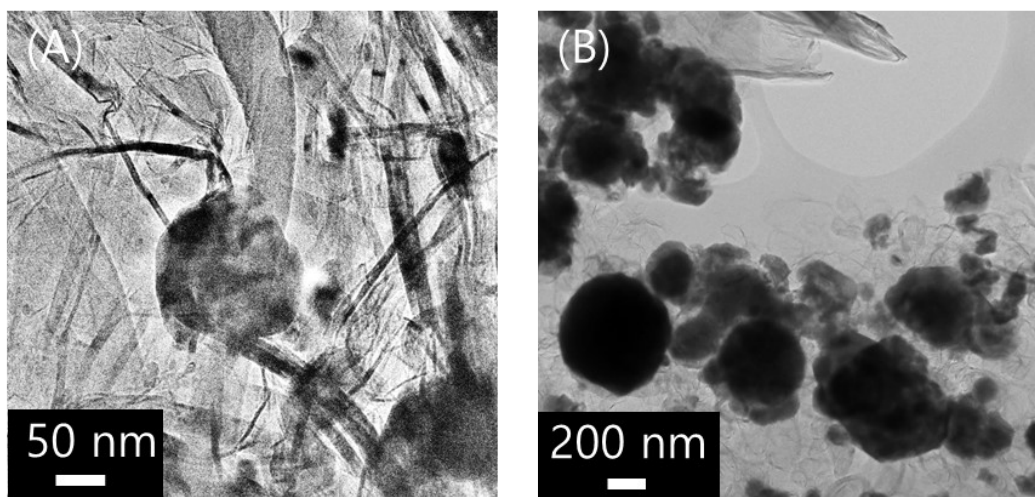


Figure S4. TEM images of (Co)Fe₃O₄-NRGO calcined at (A) 1050°C and (B) 1200°C.

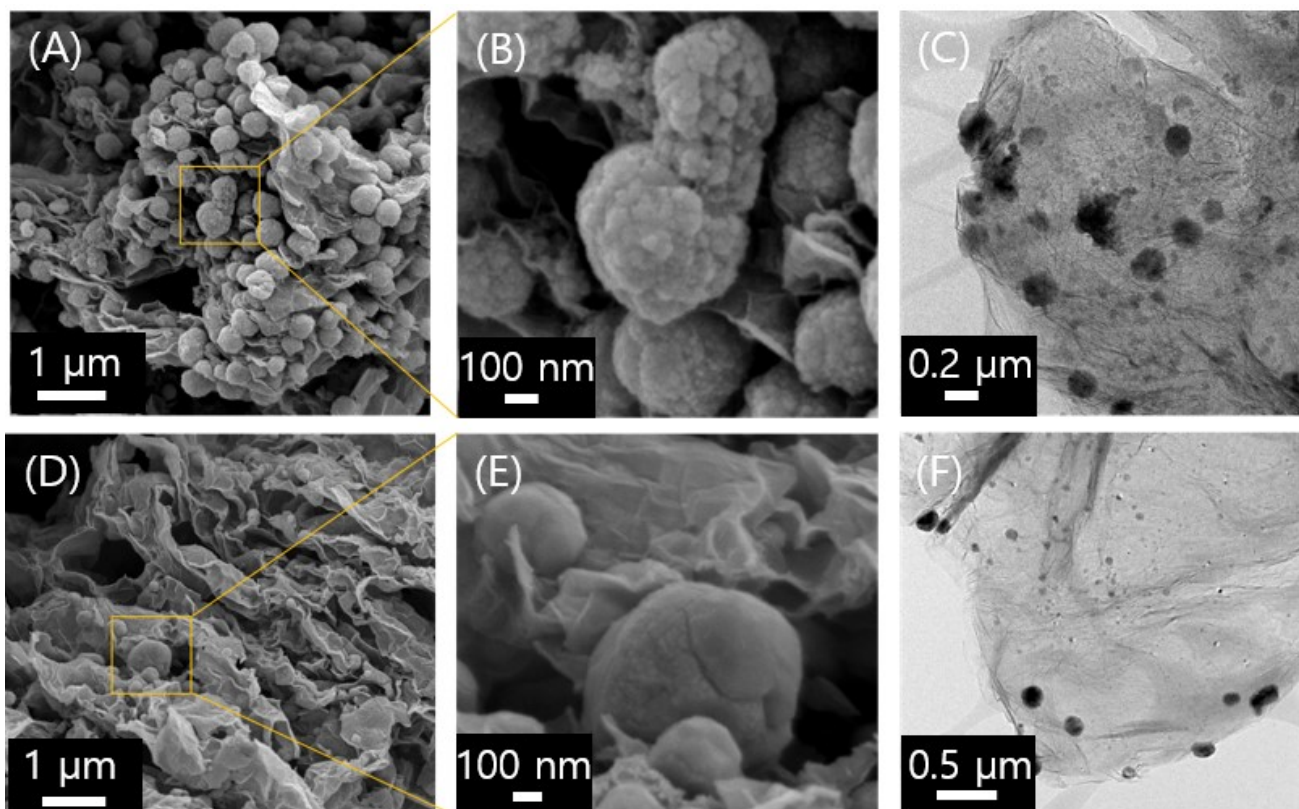


Figure S5. (A and B) SEM and (C) TEM images of Fe(OH)_x-NRGO, (D and E) SEM and (F) TEM images of FeO_x-NRGO.

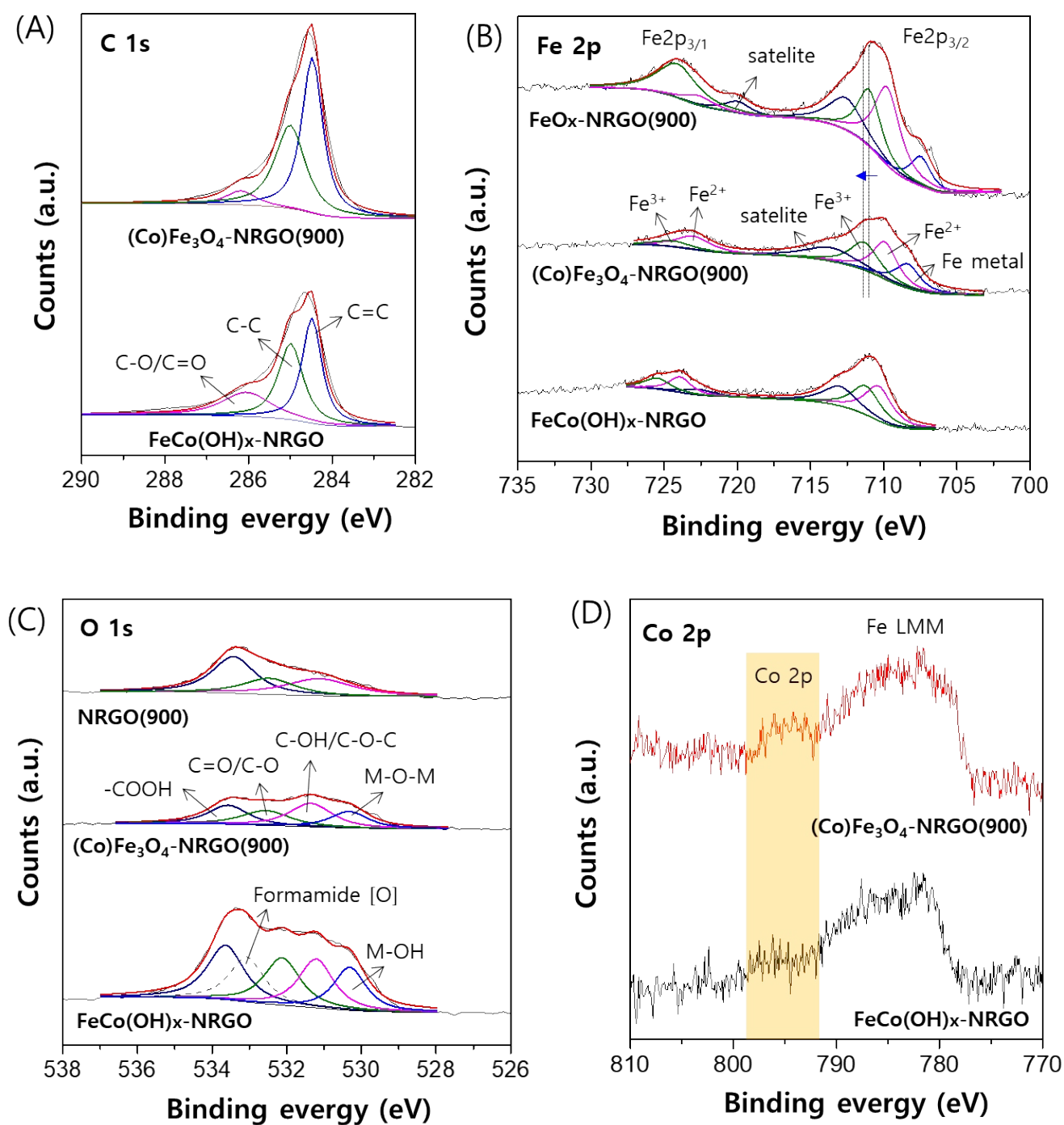


Figure S6. (A-D) XPS spectra of (A) and (D) C 1s and Co 2p of FeCo(OH)_x-NRGO and (Co)Fe₃O₄-NRGO (900), (B) Fe 2p of FeCo(OH)_x-NRGO, (Co)Fe₃O₄-NRGO (900) and FeO_x-NRGO(900), (C) O 1s of NRGO(900), FeCo(OH)_x-NRGO and (Co)Fe₃O₄-NRGO (900).

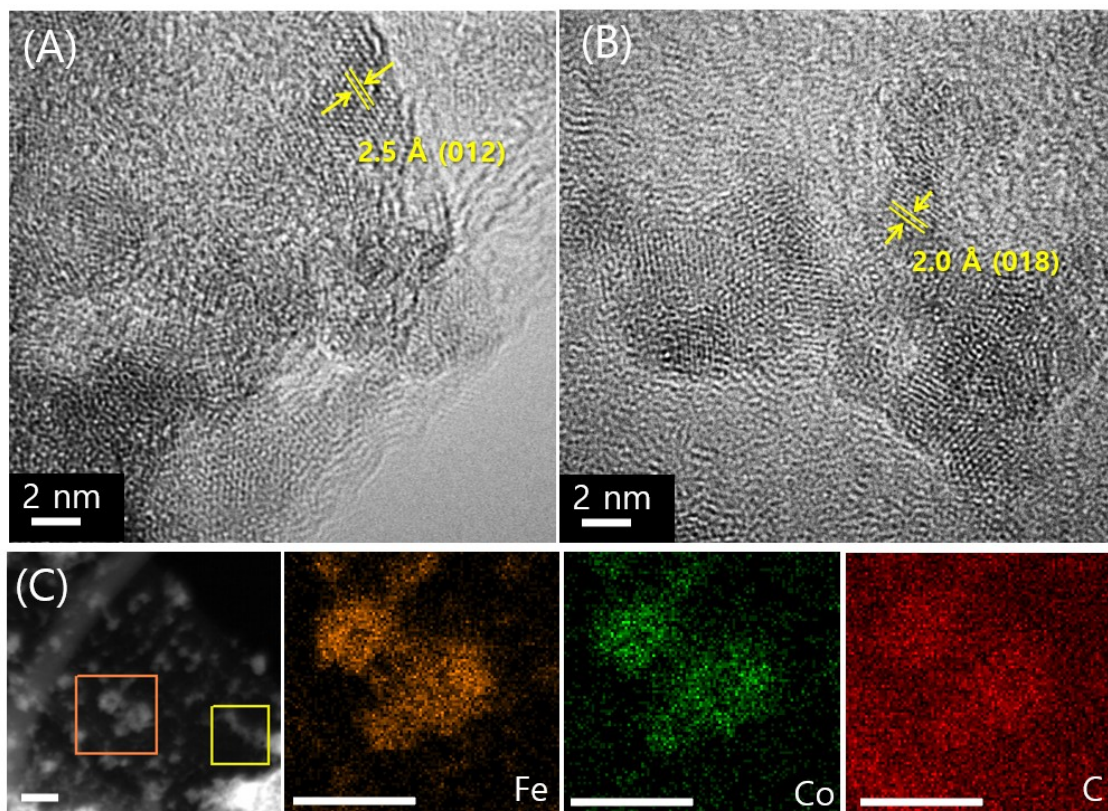


Figure S7. (A and B) HR-TEM and (C) elemental mapping images of $\text{FeCo(OH)}_x\text{-NRGO}$, the orange box area represents EDX mapping region. (The scale bar is 50 nm)

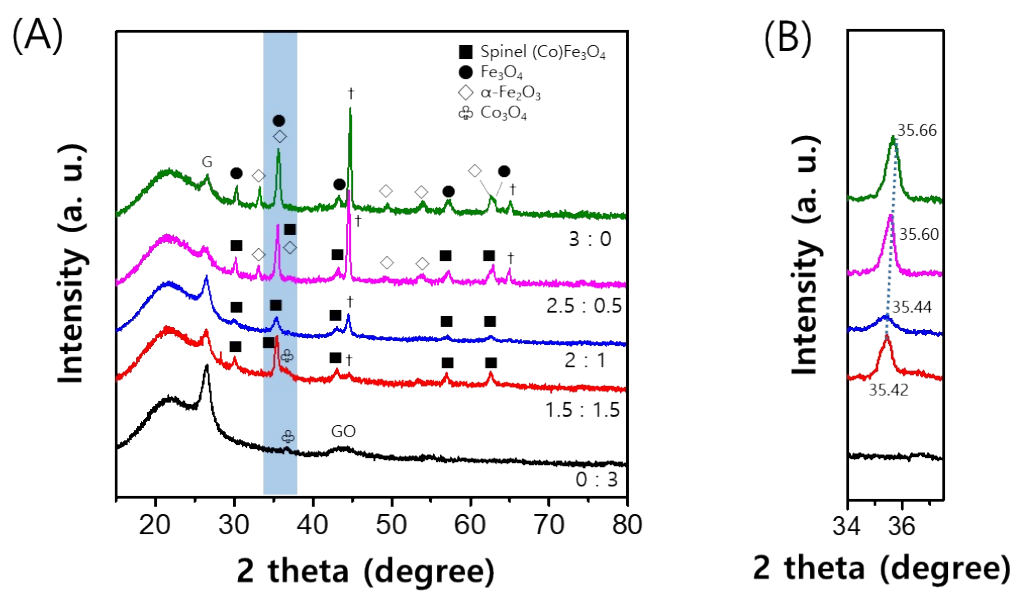


Figure S8. (A) XRD patterns of the post-calcination products corresponding to the expected Fe:Co ratios in the reactant. (B) Enlarged view of the 34-36° region from panel (A).

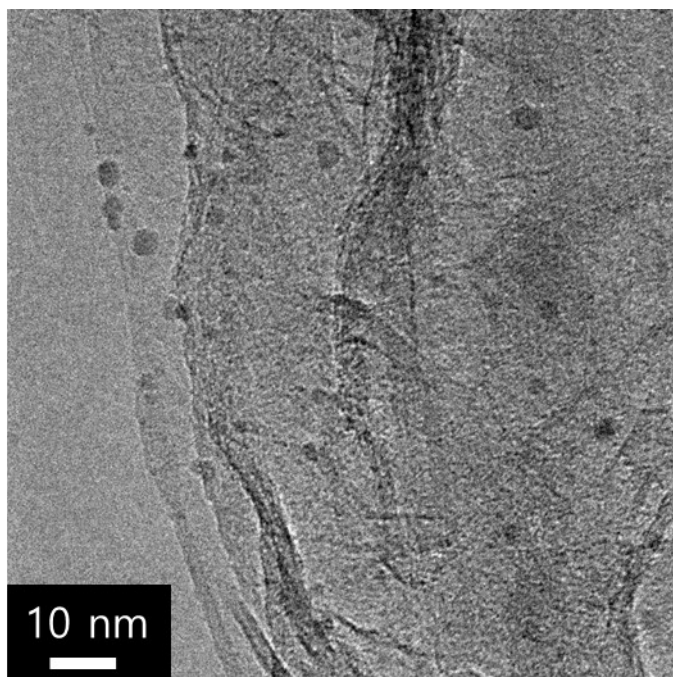


Figure S9. A TEM image depicting Co₃O₄-NRGO obtained when only Co ions were added, excluding Fe ions, at a ratio of 0:3 as shown in Figure S7.

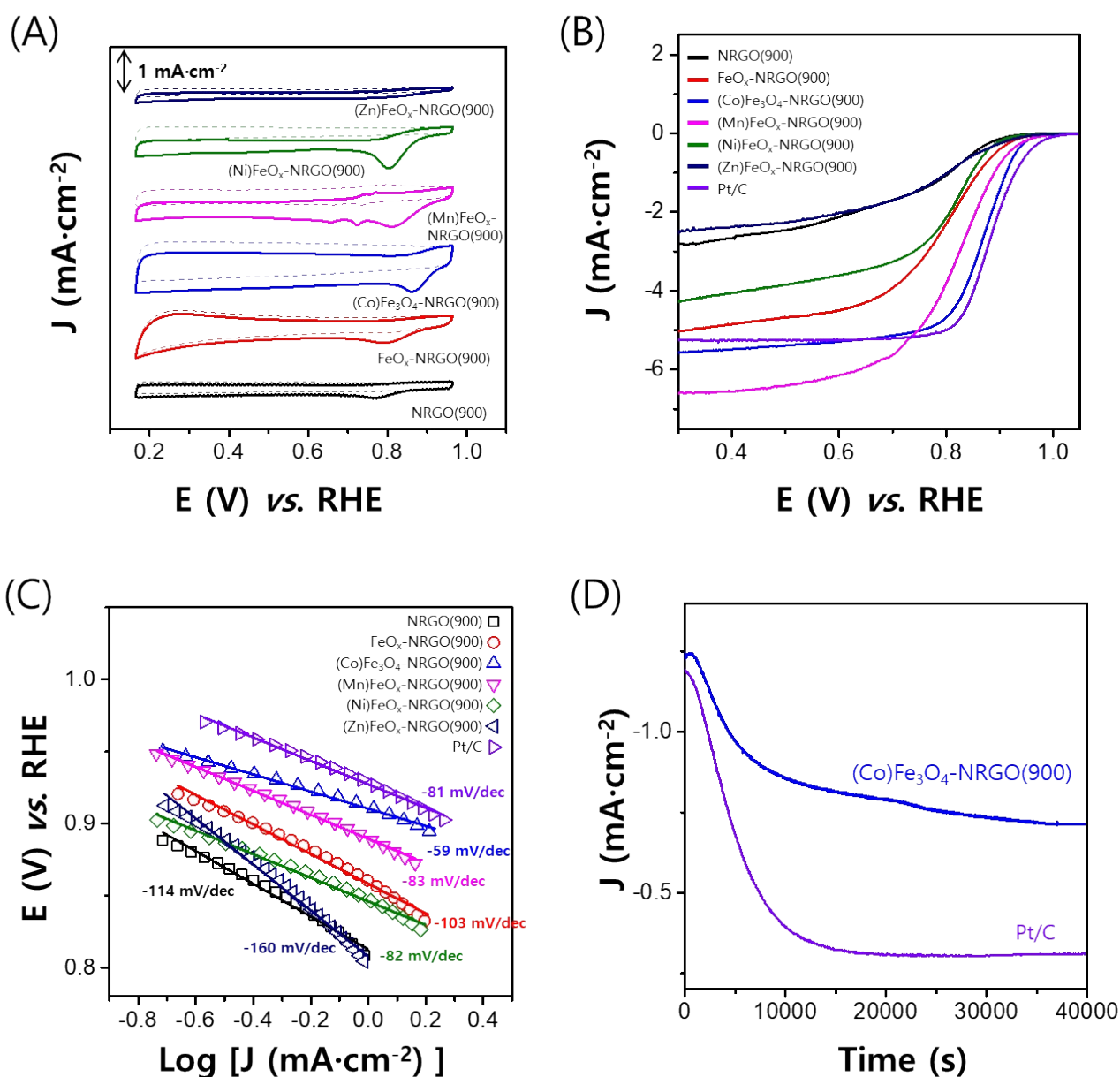


Figure S10. ORR polarization curves and kinetics of the electrochemical catalysis. (A) CV, (B) LSV curves and (C) Tafel plots of GC electrodes modified with NRGO(900), FeO_x-NRGO(900), (Co)Fe₃O₄-NRGO, (Mn)FeO_x-NRGO, (Ni)FeO_x-NRGO, (Zn)FeO_x-NRGO, and Pt/C. The CV curves were measured in 60 mL of 0.1 M KOH electrolyte solution under O₂-saturated conditions (solid line) and N₂-saturated conditions (dashed line) at a scan rate of 25 mV/s. The LSV curves were measured in the same electrolyte solution at a scan rate of 5 mV/s with a rotation rate of 1600 rpm. (D) Comparison of chronoamperometric responses for the ORR at 0.75 V with a rotation rate of 200 rpm for 50000 s for (Co)Fe₃O₄-NRGO(900) and commercial Pt/C.

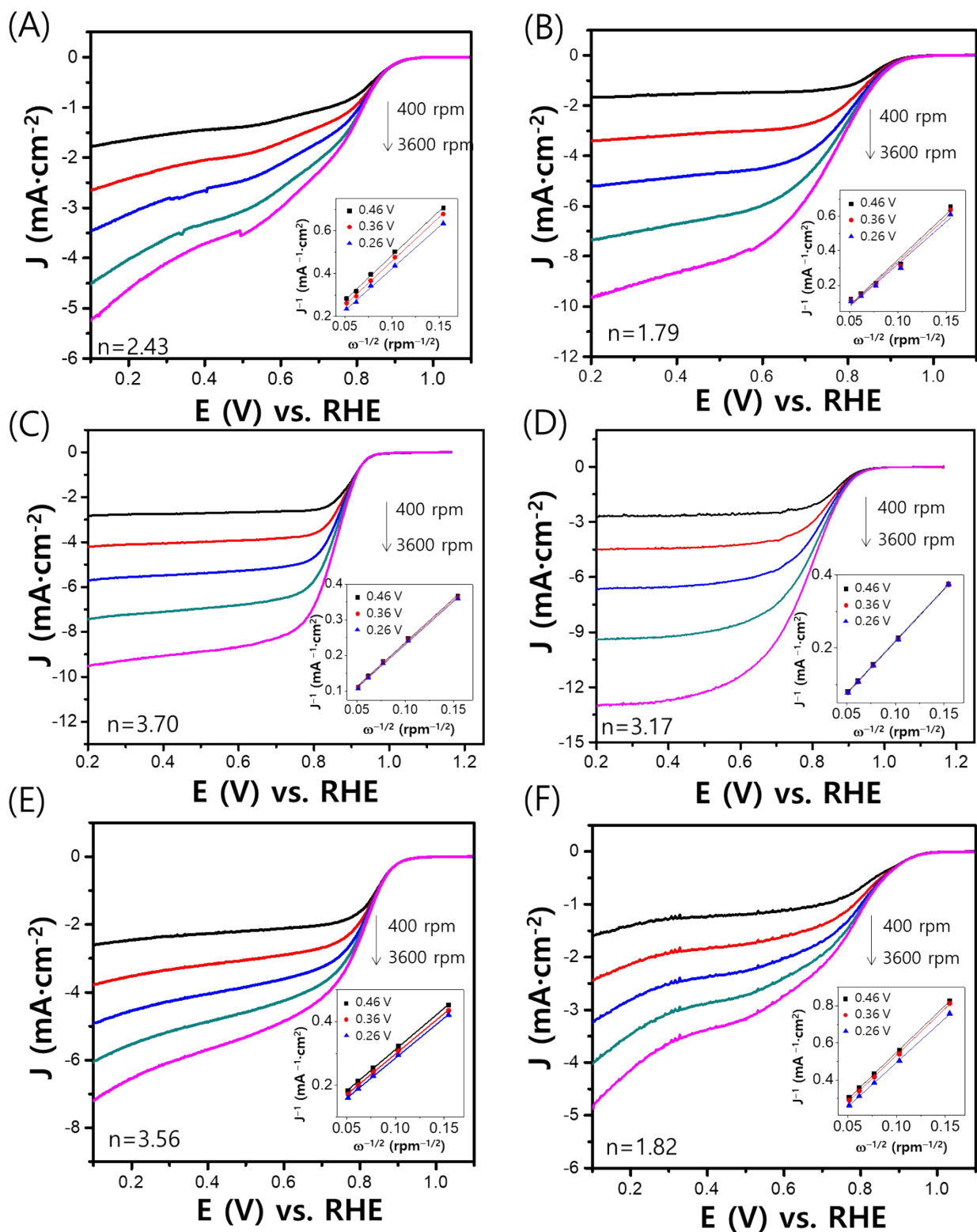


Figure S11. ORR polarization curves at different rotation rates (400-3600 rpm) for glassy carbon (GC) electrodes modified with: (A) NRGO(900), (B) FeO_x -NRGO(900), (C) $(\text{Co})\text{Fe}_3\text{O}_4$ -NRGO, (D) $(\text{Mn})\text{FeO}_x$ -NRGO, (E) $(\text{Ni})\text{FeO}_x$ -NRGO, (F) $(\text{Zn})\text{FeO}_x$ -NRGO. The insets depict the corresponding K-L plots derived from the ORR polarization curves.

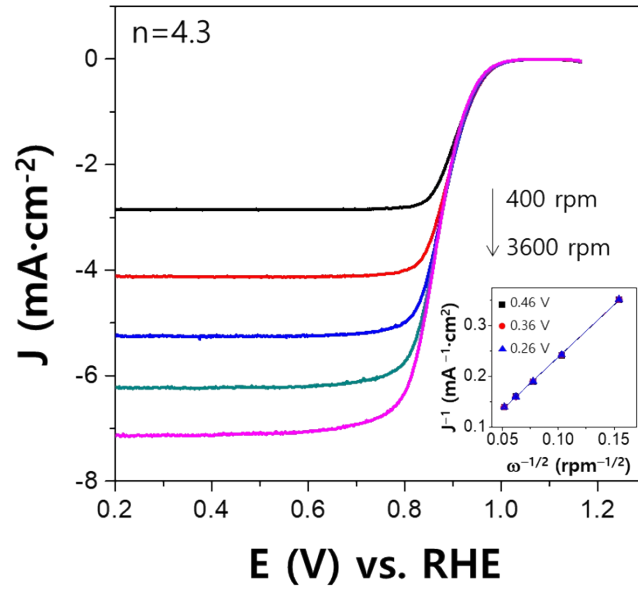


Figure S12. ORR polarization curves at different rotation rates (400-3600 rpm) for glassy carbon (GC) electrodes modified with commercial Pt/C. The insets depict the corresponding K–L plots derived from the ORR polarization curves.

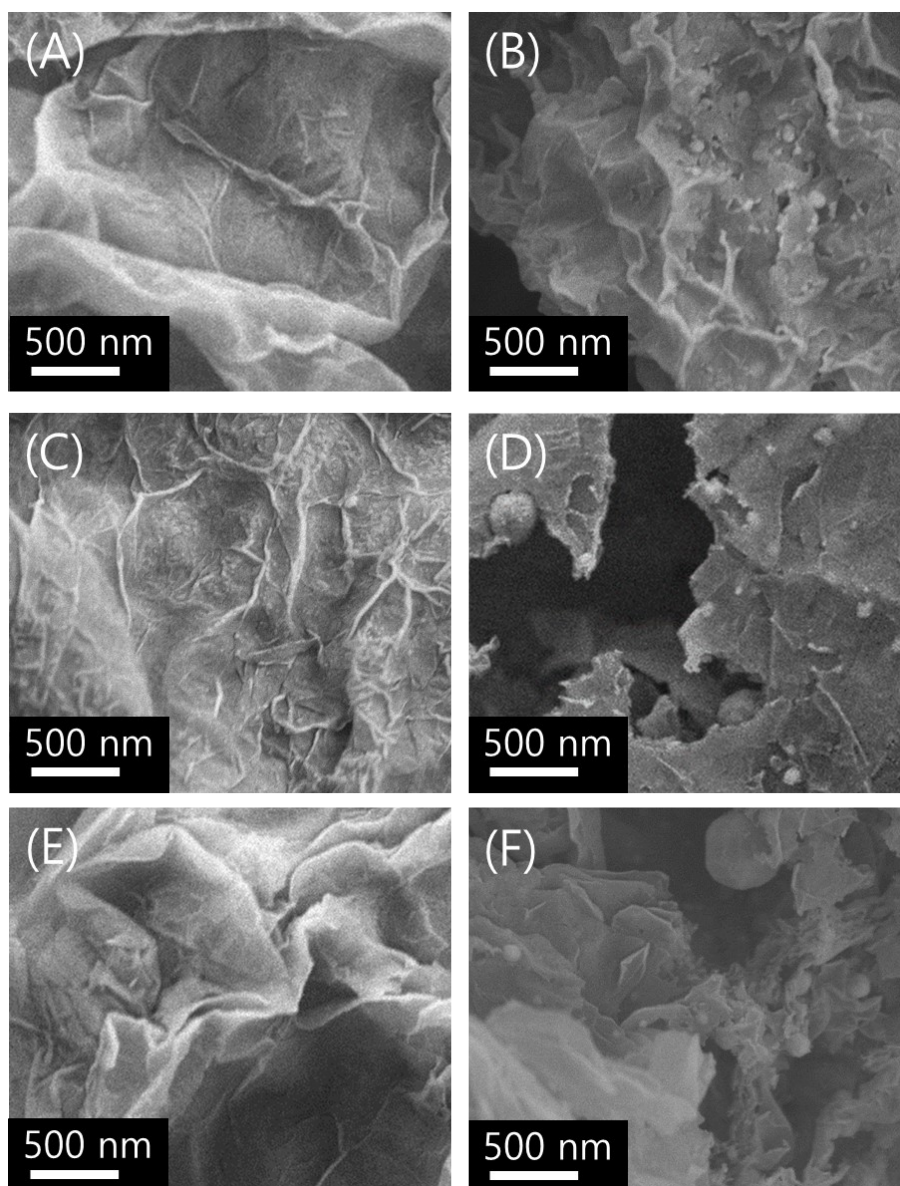


Figure S13. (A-F) SEM images showing the addition of (A, C, and E) MnCl_2 , NiCl_2 , and ZnCl_2 to the solvothermal NRGO samples and (B, D, and F) the same samples after the calcination process of $(\text{Mn})\text{FeO}_x\text{-NRGO}$, $(\text{Ni})\text{FeO}_x\text{-NRGO}$, and $(\text{Zn})\text{FeO}_x\text{-NRGO}$ at 900°C .

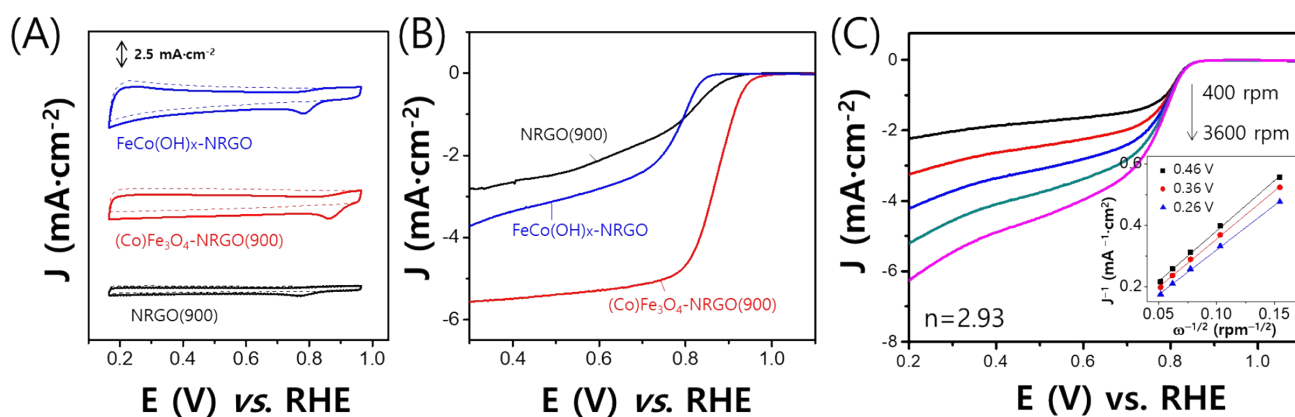


Figure S14. ORR polarization curves and kinetics of the electrochemical catalysis. (A) CV, (B) LSV curves, and (C) LSV curves at different rotation rates (400-3600 rpm) for FeCo(OH)_x-NRGO, for comparison of the pre-calcination sample of (Co)Fe₃O₄-NRGO(900). In Figure S12(C), the insets depict the corresponding K–L plots derived from the ORR polarization curves of FeCo(OH)_x-NRGO.

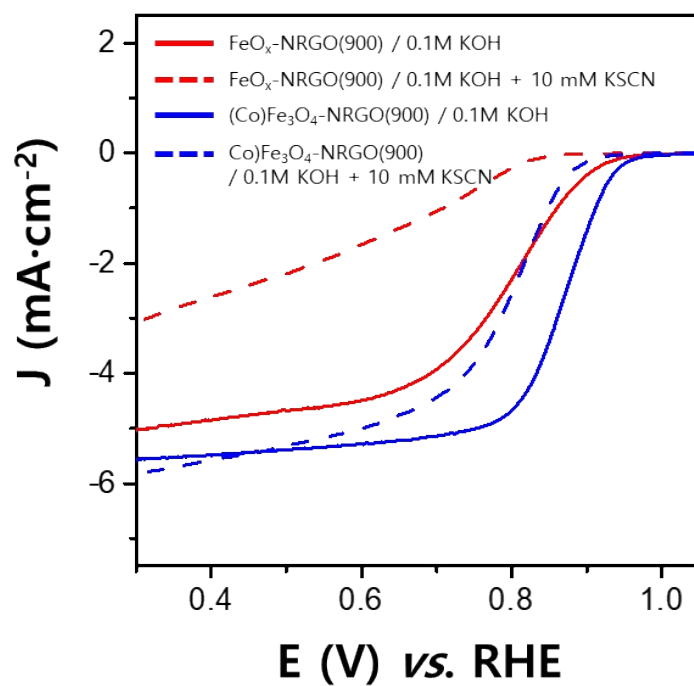


Figure S15. LSV curves of KSCN poisoned FeO_x-NRGO(900) and (Co)Fe₃O₄-NRGO(900) in 0.1 M KOH.

Table S1. Summary of onset potentials and half-wave potentials. The onset potentials of LSV curves were determined using the tangent method [4-5].

Samples	Onset potentials (V)	Half-wave potentials (V)
NRGO(900)	0.89	0.82
FeO _x -NRGO(900)	0.91	0.81
(Co)Fe ₃ O ₄ -NRGO(900)	0.95	0.86
(Mn)FeO _x -NRGO(900)	0.93	0.83
(Ni)FeO _x -NRGO(900)	0.90	0.83
(Zn)FeO _x -NRGO(900)	0.88	0.80
FeCo(OH) _x -NRGO	0.84	0.80
Pt/C	0.99	0.87

The data supporting this article have been included as part of the Electronic Supplementary Information (ESI). The ESI file 'SupplementaryData' contains analysis scripts, and additional figures used in this study.

The datasets used and/or analysed during the current study available from the corresponding author on reasonable request.

References

1. S. Kwon and J. H. Lee, *Bull. Korean Chem. Soc.*, 2021, **42**, 786-791.
2. S. Kwon and J. H. Lee, *Dalton Trans.*, 2020, **49**, 1652-1659.
3. S. Kwon, H. T. Lee and J. H. Lee, *Chem. - Eur. J.*, 2020, **26**, 14359-14365.
4. T.-N. Tran, M. Y. Song, K. P. Singh, D.-S. Yang and J.-S. Yu, *J. Mater. Chem. A*, 2016, **4**, 8645-8657.
5. A. Ilnicka, P. Kamedulski, M. Skorupska and J. P. Lukaszewicz, *J. Mater. Sci.*, 2019, **54**, 14859-14871.